ISSN 1063-7761, Journal of Experimental and Theoretical Physics, 2019, Vol. 129, No. 4, pp. 710–721. © Pleiades Publishing, Inc., 2019.
Russian Text © The Author(s), 2019, published in Zhurnal Eksperimental'noi i Teoreticheskoi Fiziki, 2019, Vol. 156, No. 4, pp. 761–774.

Contribution for the JETP special issue in honor of I. M. Khalatnikov's 100th anniversary

Theory of Dynamical Systems and Transport Phenomena in Normal Metals

S. P. Novikov[a,b], R. De Leo[c], I. A. Dynnikov[b], and A. Ya. Maltsev[a,*]

[a] *Landau Institute for Theoretical Physics, Russian Academy of Sciences, Chernogolovka, Moscow oblast, 142432 Russia*
[b] *Steklov Mathematical Institute, Russian Academy of Sciences, Moscow, 119991 Russia*
[c] *Department of Mathematics, Howard University, Washington, DC 20059 USA*
**e-mail: maltsev@itp.ac.ru*

Received March 18, 2019; revised March 18, 2019; accepted March 19, 2019

Abstract—The results of recent studies in the theory of dynamical systems related to the motion of electrons on complex Fermi surfaces in normal metals are presented. The problem considered is closely related to the description of electron transport phenomena in strong magnetic fields and is therefore of great interest from the viewpoint of topology and dynamical systems theory. We will try to give a brief overview of the state of the art in this research area, as well as point out a number of interesting issues that are being actively studied at present.

DOI: 10.1134/S106377611910008X

1. INTRODUCTION

We would like to provide an overview of the state of the art in the research field that emerged in the 1950s–1960s in the scientific school of I.M. Lifshitz, which in those years had close links with the Landau Institute for Theoretical Physics. Namely, we will consider issues related to the features of transport phenomena in metals with complex Fermi surfaces in the presence of strong magnetic fields. As a rule, as the main example of such phenomena, one considers galvanomagnetic phenomena in normal metals, although everything discussed below is also related to other types of such phenomena (for example, thermal transport phenomena). The kinetic description of electronic processes based on the quasiclassical approximation for electron dynamics in a crystal serves as the main approximation to the description of the phenomena under consideration. It turns out that the quasiclassical description of the dynamics of electronic states in the quasimomentum space may be extremely nontrivial for metals with complex Fermi surfaces. Here we would like to present the results of investigations of the corresponding dynamic problem, which have been carried out over the past decades with the use of the most modern methods of topology and dynamical systems theory. Below, we will see from the results presented that, currently, most of the most important aspects of the problem have been studied in great detail, which makes it possible to give a very detailed description of the physical phenomena associated with this problem. At the same time, we can also point out a number of interesting problems that are related to the problem under consideration and are being actively studied.

Everything presented below applies to metals with complex Fermi surfaces, and metal samples are assumed to be single-crystal and sufficiently pure and have a sufficiently low temperature, so that the electron mean free time τ in a metal can be assumed to be quite large. A metal sample is assumed to be placed in a constant external magnetic field whose value satisfies the condition $\omega_B\tau \gg 1$, where $\omega = eB/m^*c$ plays the role of the electron cyclotron frequency in the metal. We should say that, in fact, both quantities $m^* \approx p_F/v_F$ and ω_B have a somewhat formal meaning here, since the electron spectrum in the crystal is generally defined by an arbitrary 3-periodic function $\epsilon(\mathbf{p})$ with periods equal to the periods of the reciprocal lattice. A change in the electronic state in the presence of a magnetic field is defined by an adiabatic system in the quasimomentum space (see, for example, [1–3]),

$$\dot{\mathbf{p}} = \frac{e}{c}[\mathbf{v}_{\mathrm{gr}}(\mathbf{p}) \times \mathbf{B}] \equiv \frac{e}{c}[\nabla\epsilon(\mathbf{p}) \times \mathbf{B}] \qquad (1.1)$$

which has, generally speaking, trajectories of the most diverse geometry (which is the main topic discussed in this paper). One can say that the magnetic field B is strong enough if the electron has time to pass many

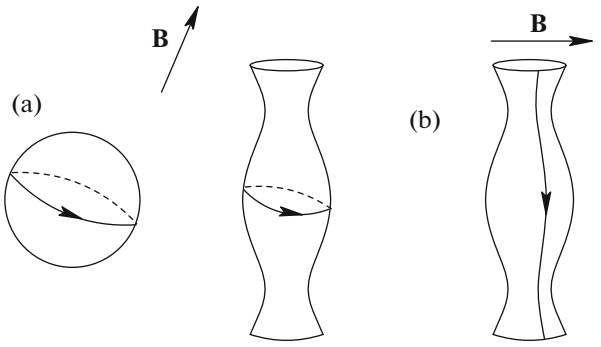

Fig. 1. (a) Closed (a) and (b) periodic trajectories of system (1.1) arising on Fermi surfaces of various shapes.

times along typical closed trajectories of system (1.1) or if it travels a sufficiently large distance ($\gg p_F$) along open trajectories of the same system between two impurity scattering events.

As is easy to see, system (1.1) preserves both the value of the electronic state energy $\epsilon(\mathbf{p})$ and the projection of the quasimomentum along the magnetic field. As a consequence, the trajectories of systems (1.1) in the $\mathbf{p}$-space are defined geometrically by the intersections of surfaces of constant energy $\epsilon(\mathbf{p}) = \text{const}$ with planes orthogonal to the magnetic field.

We can also write a quasiclassical system describing the motion of an electron wave packet in the coordinate space,

$$\dot{\mathbf{x}} = \mathbf{v}_{\text{gr}}(\mathbf{p}) \equiv \nabla\epsilon(\mathbf{p}). \tag{1.2}$$

It is also easy to see that the trajectories of system (1.2) are actually determined by the trajectories of system (1.1); in particular, their projections onto a plane orthogonal to $\mathbf{B}$ are similar to the trajectories of system (1.1) rotated through 90°. The trajectories of system (1.2) are not generally planar and describe also the motion along the direction of $\mathbf{B}$, which is determined by the corresponding values of the group velocity $\mathbf{v}_{\text{gr}}(\mathbf{p})$.

The key role in the analysis of electron transport phenomena in metals is played by the Fermi surface, which is defined by the equation

$$\epsilon(\mathbf{p}) = \epsilon_F$$

and represents a 3-periodic surface in the $\mathbf{p}$-space. Thus, one can see that the complexity in the behavior of transport phenomena in strong magnetic fields is mostly determined by the complexity of the Fermi surface of the metal. This quite important property of transport phenomena in strong magnetic fields was first pointed out in the pioneer work [4], where the authors considered two fundamentally different types of trajectories of system (1.1) on different Fermi surfaces. Namely, in [4], the authors considered contributions to the magnetoconductivity from closed and periodic trajectories of system (1.1) (Fig. 1) and showed that, in the leading order in the parameter $\omega_B\tau \gg 1$, they can be represented as

$$\sigma^{kl} \approx \frac{ne^2\tau}{m^*}\begin{pmatrix} (\omega_B\tau)^{-2} & (\omega_B\tau)^{-1} & (\omega_B\tau)^{-1} \\ (\omega_B\tau)^{-1} & (\omega_B\tau)^{-2} & (\omega_B\tau)^{-1} \\ (\omega_B\tau)^{-1} & (\omega_B\tau)^{-1} & * \end{pmatrix}, \quad \omega_B\tau \to \infty \tag{1.3}$$

(closed trajectories) and

$$\sigma^{kl} \approx \frac{ne^2\tau}{m^*}\begin{pmatrix} (\omega_B\tau)^{-2} & (\omega_B\tau)^{-1} & (\omega_B\tau)^{-1} \\ (\omega_B\tau)^{-1} & * & * \\ (\omega_B\tau)^{-1} & * & * \end{pmatrix}, \quad \omega_B\tau \to \infty \tag{1.4}$$

(open periodic trajectories).

Formulas (1.3) and (1.4) represent the orders of magnitude of $\sigma^{kl}(B)$ in the limit as $\omega_B\tau \to \infty$. In particular, it is assumed that each matrix element has in fact a certain constant dimensionless coefficient, just as the notations "*" represent some dimensionless quantities of the order of one. It is easily seen that the main difference between the contributions of closed and periodic trajectories in the limit as $\omega_B\tau \to \infty$ is the strong anisotropy of conductivity in the plane orthogonal to $\mathbf{B}$ in the second case. Henceforth, we will assume that the z axis is chosen along the magnetic field direction. In formula (1.4) we also assume that the x axis is chosen along the mean direction of periodic open trajectories in the $\mathbf{p}$-space.

In [5, 6], more general examples of open trajectories of system (1.1) were considered, which also possess strong anisotropic properties. Many issues concerning the geometry of the Fermi surface and the related physical phenomena considered in the abovementioned (as well as in a later) period were presented in [7–10], as well as in the books [1–3, 11, 12].

In the present study, we provide an overview of later results, which are based on detailed topological investigations of the structure of system (1.1) for arbitrary dispersion law $\epsilon(\mathbf{p})$ and magnetic field direction. The problem of complete classification of all possible trajectories of system (1.1) was first posed by Novikov in [13], where he also carried out the first analyses of this system in the general statement. During subsequent decades, this problem was intensively investigated in the topological school of Novikov (S.P. Novikov, A.V. Zorich, S.P. Tsarev, and I.A. Dynnikov), which produced a number of rather deep mathematical results that have allowed one to answer most of important questions related to the problem.

When describing the trajectories of system (1.1), the most important role is played by the description of its stable open trajectories, which was obtained in [14–16]. Here an especially important role is actually played by the topological structure of the Fermi sur-

face that arises upon the appearance of stable open trajectories of system (1.1) and gives rise to the remarkable geometric properties of such trajectories. As pointed out in [17, 18], stable open trajectories of (1.1) also possess important topological characteristics (topological quantum numbers), which are directly observed in transport phenomena in strong magnetic fields. In this case, the corresponding topological characteristics are expressed by integers and are locally stable under small variations of the magnetic field direction. In the most general case, all stable open trajectories for a given Fermi surface (or for the whole dispersion law [19]) can in fact be divided into families corresponding to different values of the above-mentioned topological characteristics and represented by certain stability zones on the diagram of magnetic field directions. The general structure of the stability zones on the angular conductivity diagram of a metal may be quite nontrivial, which generally leads to a wide variety of phenomena observed experimentally (see, for example, [19–32]). In the next section, we will try to present the possibly most detailed overview of questions related to the behavior of stable open trajectories of system (1.1), as well as physical phenomena attributed to the different structure of angular diagrams for metals with arbitrary Fermi surfaces.

However, stable open trajectories are not the only example of nontrivial trajectories of system (1.1); on sufficiently complex Fermi surfaces, there may appear trajectories of absolutely different type, that exhibit much more complex (chaotic) behavior both on the Fermi surface and in the covering **p**-space. The first example of such trajectories was constructed by Tsarev [33]. It should be said that the trajectories constructed by Tsarev also have their specific features and actually form a separate class of open trajectories of system (1.1), which represents a significant part of the general classification of its trajectories.

Still more complex examples of chaotic trajectories appearing on sufficiently complex Fermi surfaces were constructed by Dynnikov [34]. Dynnikov-type trajectories exhibit the most complex behavior, which also clearly manifests itself in electron transport phenomena in strong magnetic fields (see [35, 36]). Today, the general properties of Dynnikov's chaotic trajectories, as well as the structure of the sets on which they arise, are the subject of intensive study in the theory of dynamical systems (see [37–53]). Just as Tsarev's trajectories, Dynnikov's trajectories can be related to a special class of trajectories of system (1.1) that represents an important component in the general classification of all of its trajectories. In Section 3, we give an overview of the results concerning the chaotic trajectories of system (1.1) and the related physical phenomena in strong magnetic fields.

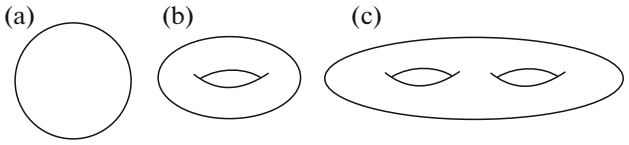

Fig. 2. Canonical compact surfaces having genera 0 (a), 1 (b), 2 (c), etc.

2. STABLE OPEN TRAJECTORIES AND ANGULAR CONDUCTIVITY DIAGRAMS OF METALS

We begin this section with the description of the structure of the Fermi surface when stable open trajectories of system (1.1) arise on it. Note, first of all, that the Fermi surface can be considered in two ways. Namely, on the one hand, the Fermi surface can be considered as a 3-periodic surface in the **p**-space, defined by the equation $\epsilon(\mathbf{p}) = \epsilon_F$. Here we should keep in mind, however, that the points of the Fermi surface differing by reciprocal lattice vectors define the same electronic state. On the other hand, the **p**-space and the Fermi surface can be factorized with respect to the reciprocal lattice vectors and considered as compact manifolds. In this case, the complete Brillouin zone represents a three-dimensional torus $\mathbb{T}^3$, and the Fermi surface represents a smooth compact two-dimensional surface S_F embedded in $\mathbb{T}^3$. As an abstract compact surface, the Fermi surface has a fixed genus $g \geq 0$ and is diffeomorphic to the canonical two-dimensional surface of appropriate genus (Fig. 2). Moreover, the embedding of the Fermi surface in $\mathbb{T}^3$ (or its representation as a periodic surface in the **p**-space) can be characterized by a topological rank that can take the values 0, 1, 2, or 3 (Fig. 3). Here we will primarily focus on the most complex Fermi surfaces; therefore, we will assume, as a rule, that the Fermi surface considered has rank 3. We can also show that the genus of such a surface should satisfy the relation $g \geq 3$.

First of all, we remove all closed (singular and nonsingular) trajectories of system (1.1) from the Fermi surface and consider its remaining part, which carries open trajectories. In the general case, all nonsingular closed trajectories of (1.1) on the Fermi surface form a finite number of (nonequivalent) cylinders bounded by singular trajectories of (1.1) on their bases (a particular case of such a base can be given by a single singular point of system (1.1)). After such a removal, the remaining part of the Fermi surface is represented by a finite number of (nonequivalent) components with holes, bounded by singular trajectories of system (1.1). We can call the set of two-dimensional components with holes thus obtained a reduced Fermi surface corresponding to a given direction of the magnetic field.

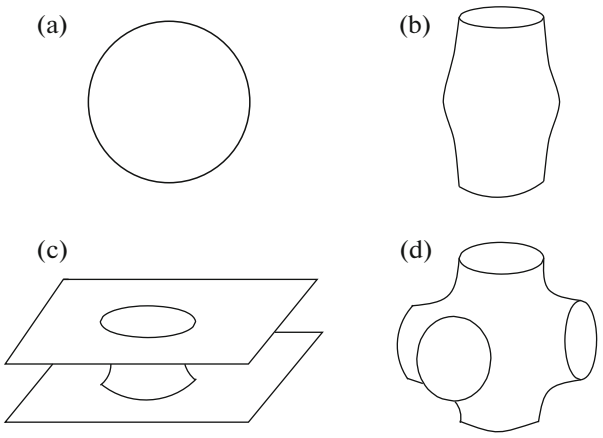

Fig. 3. Examples of Fermi surfaces in the **p**-space of rank 0 (a), 1 (b), 2 (c), and 3 (d).

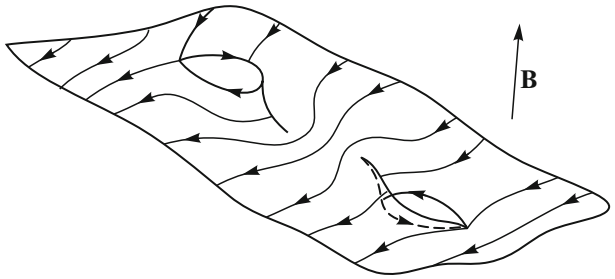

Fig. 4. Connected component of the reduced Fermi surface in the **p**-space, that carries stable open trajectories of system (1.1).

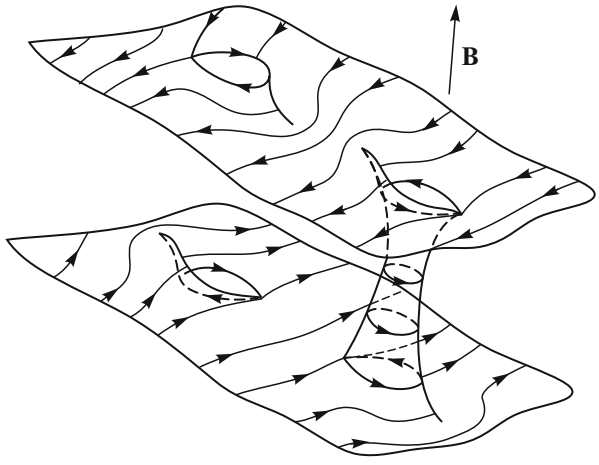

Fig. 5. General structure of the Fermi surface in the **p**-space, that carries stable open trajectories of system (1.1) (schematically).

When describing stable open trajectories of system (1.1), we can assume that the direction of **B** is completely irrational, i.e., that a plane orthogonal to **B** does not contain reciprocal lattice vectors. The most important property of the reduced Fermi surface in the presence of stable open trajectories of system (1.1) is the fact that each of its connected components represents a two-dimensional torus with holes, embedded in $\mathbb{T}^3$ [14, 16]. Returning to the extended **p**-space, we can also formulate these properties as follows: Each connected component of the reduced Fermi surface represents an integral (generated by two vectors of the reciprocal lattice) periodically deformed plane with holes, embedded in $\mathbb{R}^3$ (Fig. 4).

On the whole, the complete Fermi surface in the situation described can be represented in the general case as a set of an even number of (nonequivalent) integral planes in the **p**-space, connected by components consisting of cylinders of closed trajectories of system (1.1) of finite height (Fig. 5). Such a structure of the Fermi surface is locally stable with respect to small rotations of the direction of **B**, as well as with respect to small variations of the Fermi level ϵ_F. In this case, the Fermi surface will have the above-described different representations for the directions of **B** lying in different stability zones on the angular diagram (on the unit sphere $\mathbb{S}^2$).

As regards the stable open trajectories of system (1.1), one can see that, in the situation described, these trajectories should have the following two remarkable properties:

(1) each stable open trajectory of system (1.1) (in the **p**-space) lies in a straight strip of finite width in a plane orthogonal to **B** and passes through it (Fig. 6) (see also [15]);

(2) the mean direction of all stable open trajectories is the same for a given direction of **B** and is given by the intersection of the plane orthogonal to **B** with some (locally) fixed integral plane Γ in the **p**-space.

The geometrical properties of stable open trajectories of system (1.1) are directly related to transport phenomena in a metal in strong magnetic fields. Just as in the case of periodic open trajectories, the conductivity tensor in the plane orthogonal to **B** possesses a strong anisotropy in the limit of $\omega_B\tau \to 1$. The general property of the complete conductivity tensor

$$\sigma^{ik} \approx \frac{ne^2\tau}{m^*}\begin{pmatrix} o(1) & o(1) & o(1) \\ o(1) & * & * \\ o(1) & * & * \end{pmatrix}, \quad \omega_B\tau \to \infty, \tag{2.1}$$

allows one to determine the mean direction of open trajectories in the **p**-space as the direction of the greatest suppression of conductivity (in the **x**-space) in the limit of $\omega_B\tau \to \infty$. The stability of open trajectories with respect to small rotations of the direction of **B** allows one to determine also the integral plane Γ as the plane containing the directions of the greatest suppression of conductivity for all directions of **B** that lie

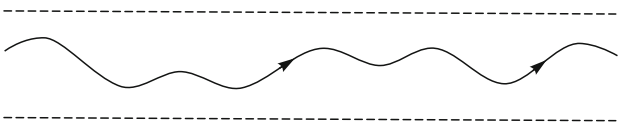

Fig. 6. View of a stable open trajectory in the plane orthogonal to **B** in the extended **p**-space.

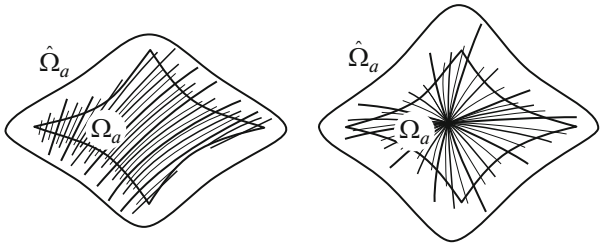

Fig. 7. Experimentally observed stability zones in experiments on direct measurements of conductivity in strong magnetic fields.

in the appropriate stability zone Ω (on the unit sphere).

The experimentally observed plane Γ is generated by some two vectors of the reciprocal lattice and, in particular, should not necessarily coincide with some crystallographic plane. Instead, it is orthogonal to a crystallographic direction of a sample and thus can be defined by an irreducible triple of integers (M^1, M^2, M^3). The integral parameters $(M^1_\alpha, M^2_\alpha, M^3_\alpha)$ of the planes Γ_α for each stability zone were introduced in [17] as important topological characteristics observed in the conductivity of normal metals. The complete set of topological numbers $(M^1_\alpha, M^2_\alpha, M^3_\alpha)$, as well as the geometry of the corresponding stability zones, represents important characteristics of the electron spectrum in a crystal. Note that a stability zone Ω_α can be defined either as a connected domain (on $\mathbb{S}^2$) corresponding to a given family of stable open trajectories of (1.1) or as a complete set of all such domains corresponding to the same integer triple $(M^1_\alpha, M^2_\alpha, M^3_\alpha)$. Quite often, it is convenient to use the second definition, which, in particular, assigns diametrically opposite domains on the unit sphere to the same zone.

Returning to the complete structure of the Fermi surface in the presence of stable open trajectories of system (1.1) on it, we can state that, as already mentioned, for the directions $\mathbf{B}/B \in \Omega_\alpha$ of general position, the Fermi surface can be represented as an even set of (nonequivalent) deformed integral planes with holes, connected by components of finite height that carry closed trajectories of system (1.1). One can also see that, in a physically realistic situation, each such component should represent a simple cylinder consisting of closed trajectories and bounded by singular trajectories on their bases (Fig. 5). Such a structure allows one to say somewhat more about the trajectories of system (1.1) for the directions of **B** lying inside some of the stability zones, as well as near it (see, for example, [19, 29–31]).

Indeed, we can note, first of all, that the given structure on the Fermi surface should give rise to periodic open trajectories for $\mathbf{B}/B \in \Omega_\alpha$ every time when the intersection of a plane orthogonal to **B** with the corresponding plane Γ_α has a rational direction in the **p**-space. As a consequence, in each zone Ω_α, one can point out an everywhere dense set (consisting of segments of large circles) of directions of **B** that corresponds to the appearance of periodic open trajectories of system (1.1). In contrast to the trajectories of general position, periodic trajectories are not everywhere dense on the carriers of open trajectories, which results in somewhat different values of conductivity for the corresponding directions of **B** in the limit of $\omega_B\tau \to \infty$. As a consequence, the angular dependence of the conductivity tensor for $\mathbf{B}/B \in \Omega_\alpha$ has a certain irregularity, which may introduce an element of randomness to the experimental data when measuring conductivity. Moreover, one can also show that, for the above-described structure of the Fermi surface, periodic open trajectories of system (1.1) also exist on the extensions of the above-mentioned segments of large circles beyond the stability zone. The latter circumstance, together with the appearance of long closed trajectories for close directions of **B**, leads to the fact that the experimentally observed stability zone $\hat{\Omega}_\alpha$ turns out to be somewhat greater in direct measurements of conductivity than the exact mathematical zone even in sufficiently strong magnetic fields (Fig. 7). On the whole, the analytic properties of the conductivity tensor in the experimentally observed stability zone may be sufficiently complex (see [29]).

At the same time, the boundaries of exact mathematical stability zones Ω_α are also experimentally observable for an appropriate setting up of the experiment. This circumstance is due to the fact that the boundary of a zone Ω_α is related to a certain reconstruction of the trajectories of system (1.1) and to the destruction of the structure shown in Fig. 5 for the corresponding directions of **B**. Namely, on the boundary of any zone Ω_α, the height of one of the cylinders of closed trajectories connecting the carriers of open trajectories vanishes, and this cylinder subsequently disappears after the intersection with the boundary of Ω_α. The disappearance of any such cylinder of closed trajectories can be detected experimentally, for example, when investigating (classical or quantum) oscillatory phenomena in a metal in strong magnetic fields (see, for example, [30]). Below we will see that it is the structure of exact mathematical stability zones that is the most interesting for metals with complex Fermi

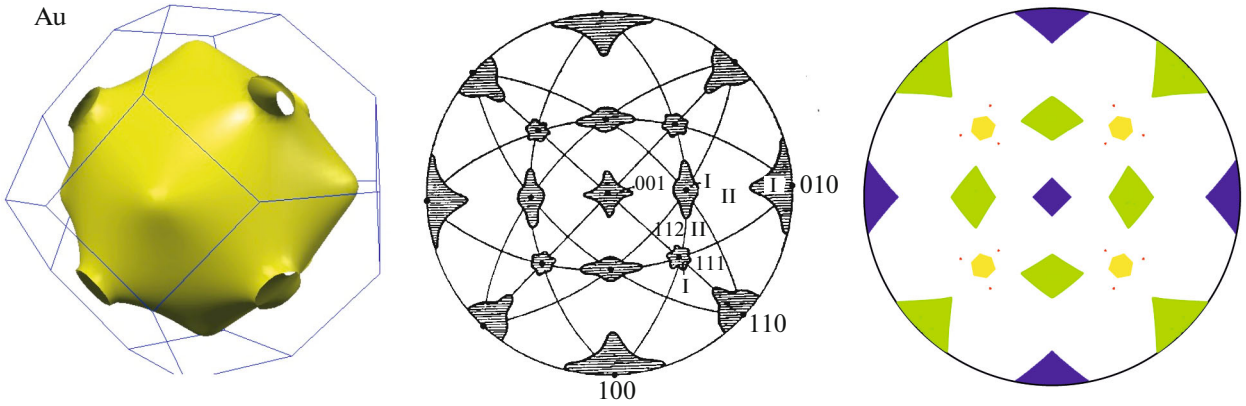

Fig. 8. (Color online) The shape of the Fermi surface of gold, experimentally measured stability zones [54], and stability zones obtained as a result of high-precision calculations [25, 26].

surfaces from the viewpoint of its mathematical description.

Another important feature of the structure shown in Fig. 5 is the fact that the intersection of the boundary of a zone Ω_α actually leads only to its partial destruction. Indeed, one can see that the disappearance of only one of the cylinders of closed trajectories does not lead to the complete disappearance of this structure, because the Fermi surface remains divided into pairs of merged-together former carriers of open trajectories separated by the remaining cylinders of closed trajectories. Thus, for the structure shown in Fig. 5 to disappear completely, it is necessary that at lest one more cylinder of closed trajectories should disappear, which makes possible the jumps of trajectories between the pairs of merged-together former carriers. Thus, one can see that, for each zone Ω_α, it is natural to introduce another (second) boundary (which, generally speaking, does not coincide with the boundary of the experimentally observed zone $\hat{\Omega}_\alpha$) corresponding to the complete disappearance of the above-described structure. In the domain Ω'_α bounded by the first and second boundaries of the zone Ω_α, the trajectories of system (1.1) also admit an effective description on the basis of the structure arising in the zone Ω_α, which also allows one to provide a description of the main physical phenomena related to the geometry of the trajectories of system (1.1) [31]. Note that, in contrast to the zones Ω_α, different zones Ω'_α and Ω'_β may intersect with each other.

The described structure of system (1.1) on the Fermi surface in the presence of stable open trajectories also provided a basis for constructing numerical methods for the analysis of this system in the general case and calculating the structure of the stability zones in especially complex examples (see, for example, [20, 24–26]). Namely, the study of the topology of the cycles defined by closed trajectories (1.1) on the Fermi surface allows one to effectively describe the global structure of trajectories even for a quite complex geometry of the Fermi surface and the presence of quite small stability zones. Figures 8 and 9 demonstrate the stability zones for the Fermi surfaces of gold and silver, obtained experimentally and calculated on the basis of the above topological methods. We can see that the numerical methods significantly improve the experimental data on the stability zones, in particular, the boundaries of experimentally measured zones. On the diagram of Fig. 8, one can see, in addition to exact stability zones determined experimentally, (very small) additional zones, which were not detected earlier in experiments.

Taking into account the possible complexity of angular conductivity diagrams, we can specially note that all nontrivial (containing stability zones) angular diagrams for normal metals can be classified into two different types [31, 32]. The type of a diagram is determined by the behavior of the Hall conductivity for the directions of **B** lying outside the stability zones; however, it is this behavior that has, as a rule, the most important impact on the general complexity of the angular diagram. More precisely, the diagrams for which the Hall conductivity has the same value everywhere outside the stability zones (for a given value of B, $\omega_B\tau \gg 1$) can be assigned to type A. Conversely, the diagrams on which there exist domains outside the stability zones with different values of the Hall conductivity (often with different, electron and hole, types of conductivity), are assigned to type B (Figs. 10 and 11). Presumably, diagrams of type A are more widespread among all diagrams for real substances; however, they are a priori simpler than diagrams of type B. In particular, a diagram of type B contains, in the general case, an infinite number of stability zones with arbitrarily large values of topological numbers, whereas, for diagrams of type A, the presence of an infinite number of stability zones is an exceptional case (see [32]).

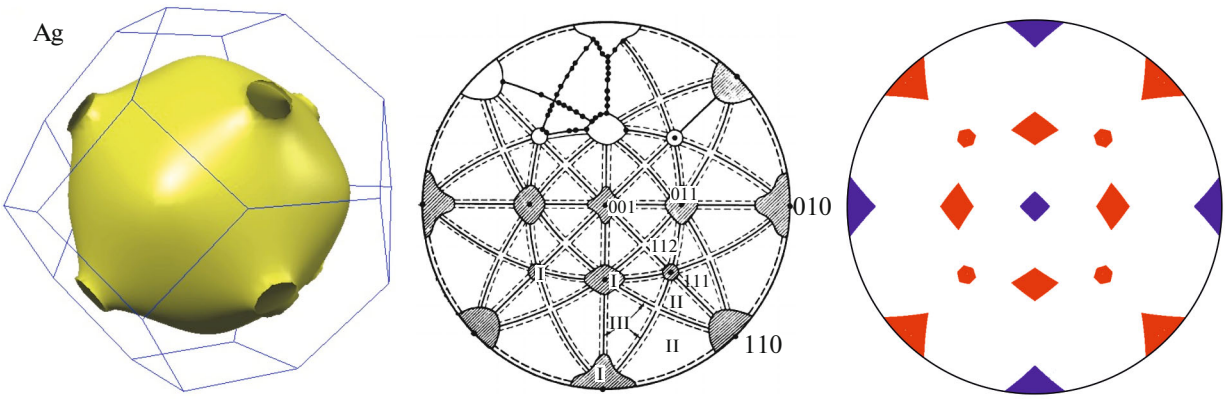

Fig. 9. (Color online) The shape of the Fermi surface of silver, experimentally measured stability zones [55], and stability zones obtained as a result of high-precision calculations [25, 26].

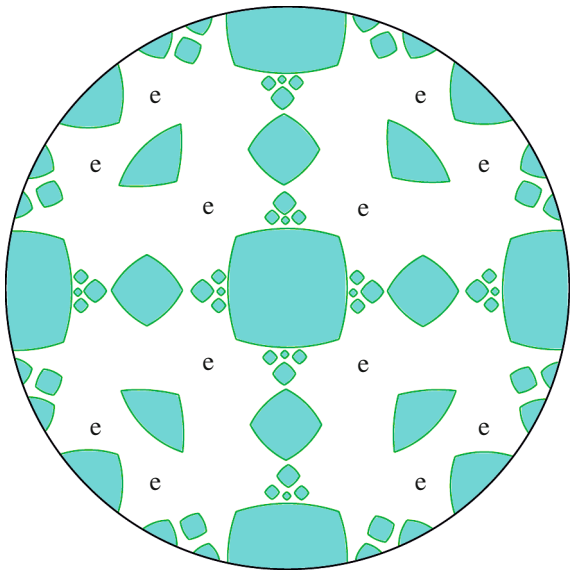

Fig. 10. (Color online) Example of an A-type diagram (very schematically) with the same (electron) type of behavior of the Hall conductivity outside the stability zones.

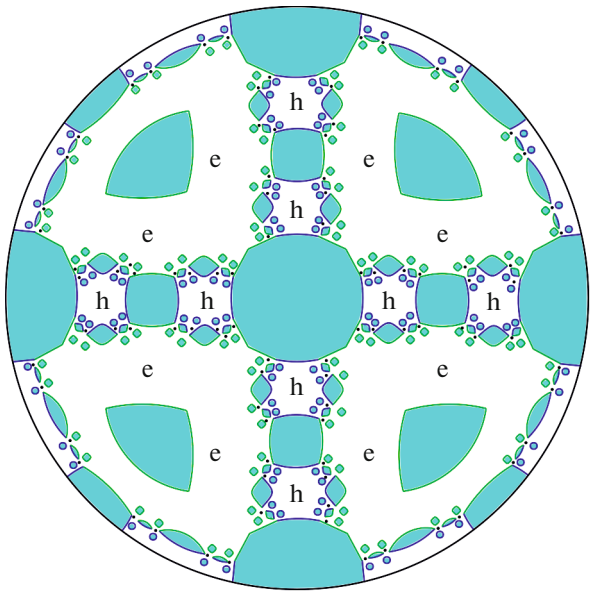

Fig. 11. (Color online) Example of a B-type diagram (only a finite number of stability zones and chaotic directions of **B** are shown very schematically) with different (electron and hole) types of the Hall conductivity in different domains outside the stability zones.

When considering stable open trajectories of system (1.1) and the corresponding stability zones in the space of directions of **B**, one should not neglect the possibility of introducing the general angular diagram for the whole dispersion relation $\epsilon(\mathbf{p})$ describing the behavior of open trajectories of (1.1) on all energy levels $\epsilon(\mathbf{p}) = \text{const}$ simultaneously [19]. The possibility of introducing such a diagram is based on the following important assertions on the trajectories of system (1.1), which were proved in [19].

Consider an arbitrary 3-periodic dispersion relation $\epsilon(\mathbf{p})$ and the corresponding systems (1.1) that arise for different directions of **B**. Then the following statements hold:

(1) for each direction of **B**, open trajectories of system (1.1) exist either in a closed energy interval $\epsilon \in [\epsilon_1(\mathbf{B}/B), \epsilon_2(\mathbf{B}/B)]$ or on a single energy level $\epsilon = \epsilon_0(\mathbf{B}/B) = \epsilon_1(\mathbf{B}/B) = \epsilon_2(\mathbf{B}/B)$;

(2) every time when open trajectories of system (1.1) arise in a finite energy interval $[\epsilon_1(\mathbf{B}/B), \epsilon_2(\mathbf{B}/B)]$, all nonsingular open trajectories lie in straight strips of finite width in the planes orthogonal to **B** and pass through these strips;

(3) for generic directions of **B**, the values of the functions $\epsilon_1(\mathbf{B}/B)$ and $\epsilon_2(\mathbf{B}/B)$ coincide with the values of some continuous functions $\tilde{\epsilon}_1(\mathbf{B}/B)$ and $\tilde{\epsilon}_2(\mathbf{B}/B)$ that are defined everywhere on the unit

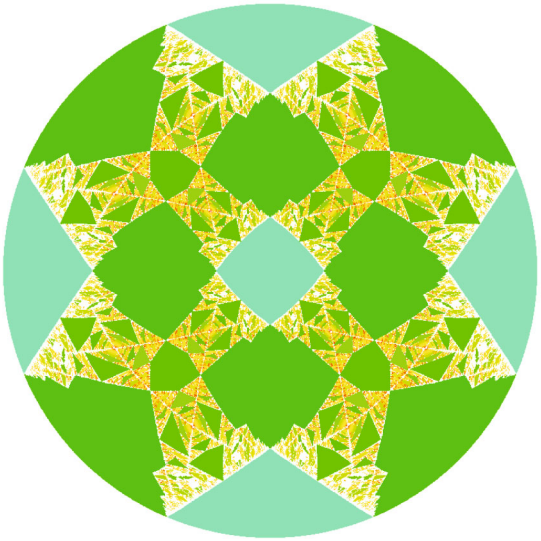

Fig. 12. (Color online) Example of a complex angular diagram for the dispersion relation $\epsilon(\mathbf{p}) = \cos x \cos y + \cos y \cos z + \cos z \cos x$ (only a finite number of stability zones are shown (in color)) in the order of increasing corresponding topological numbers [51].

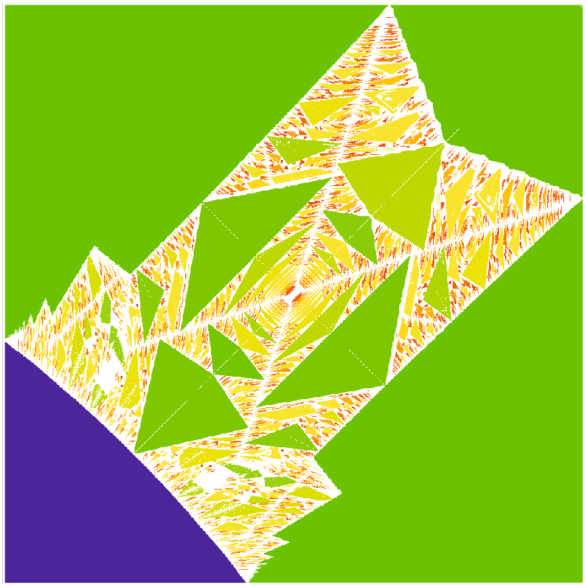

Fig. 13. (Color online) Fractal structure of the set of chaotic directions of **B** (the complement of the stability zones) on the angular diagram.

sphere $\mathbb{S}^2$. For special directions of **B** such that the plane orthogonal to **B** contains a reciprocal lattice vector, the values of $\epsilon_1(\mathbf{B}/B)$ and $\epsilon_2(\mathbf{B}/B)$ may not coincide with $\tilde{\epsilon}_1(\mathbf{B}/B)$ and $\tilde{\epsilon}_2(\mathbf{B}/B)$ (if a given direction of **B** corresponds to the appearance of periodic trajectories of system (1.1)). In this case, we always have the relations

$$\epsilon_1(\mathbf{B}/B) \le \tilde{\epsilon}_1(\mathbf{B}/B), \quad \text{and} \quad \epsilon_2(\mathbf{B}/B) \ge \tilde{\epsilon}_2(\mathbf{B}/B).$$

(4) For generic directions of **B**, such that $\tilde{\epsilon}_1(\mathbf{B}/B) < \tilde{\epsilon}_2(\mathbf{B}/B)$, all nonsingular open trajectories of (1.1) have the same mean direction in the **p**-space that is defined by the intersection of the plane orthogonal to **B** with some integral plane Γ (generated by two vectors of the reciprocal lattice) that is invariant under small rotations of the direction of **B**. Thus, the plane Γ is constant for any connected domain on $\mathbb{S}^2$ in which the relation $\tilde{\epsilon}_1(\mathbf{B}/B) < \tilde{\epsilon}_2(\mathbf{B}/B)$ is satisfied. Maximal (open) connected domains Ω_α satisfying the above condition can be called stability zones for the whole dispersion law $\epsilon(\mathbf{p})$. Each stability zone Ω_α has a piecewise constant boundary on which the relations $\tilde{\epsilon}_1(\mathbf{B}/B) = \tilde{\epsilon}_2(\mathbf{B}/B)$ are satisfied. Each stability zone Ω_α corresponds to some integral plane Γ_α defined by the above conditions.

(5) The family of all stability zones Ω_α forms an everywhere dense open set on the unit sphere $\mathbb{S}^2$.

We can also note that all angular diagrams for the dispersion relation can be divided into two classes. Namely,

(1) complex diagrams containing an infinite number of stability zones (Fig. 12) and

(2) simple diagrams containing a single stability zone that fills the whole sphere $\mathbb{S}^2$.

For complex angular diagrams described above, of great interest is also the structure of the set

$$\mathbb{S}^2 \setminus \cup \overline{\Omega_\alpha}.$$

This set represents the set of directions of **B** for which there appear chaotic trajectories of system (1.1), which we will discuss in the next chapter. The structure of this set is in fact quite complex (fractal, Fig. 13). According to the Novikov conjecture [23], for dispersion laws of general position, the Hausdorff dimension of this set is strictly less than 2.

We can see that the structure of angular diagrams for the whole dispersion law is in most cases much more complex than the structure of angular diagrams for a fixed Fermi surface. It is interesting to notice, however, that there exist special Fermi surfaces for which angular diagrams coincide with the angular diagrams for the whole dispersion law [20]. For example, such a surface is given by the surface $\cos x + \cos y + \cos z = 0$, whose angular diagram is (partially) represented in Fig. 14.

Note also that the angular diagrams for the whole dispersion law are, in some extent, abstract from the viewpoint of the theory of normal metals. It is not unlikely, however, that there is a certain possibility to observe such diagrams in semiconducting single crystals in the presence of superstrong magnetic fields [56].

3. CHAOTIC OPEN TRAJECTORIES OF SYSTEM (1.1)

Here we consider open trajectories of system (1.1) that are different from those considered in the previous section and the related physical phenomena. As we already pointed out in the Introduction, the first examples of this kind were constructed by Tsarev in 1992. Here we describe only the general properties of Tsarev's trajectories; more detailed description of these trajectories can be found, for example, in [34, 52]. Note at once that Tsarev-type trajectories represent a separate class of unstable open trajectories of system (1.1), these trajectories arise for "partially irrational" directions of **B** (the plane orthogonal to **B** contains a reciprocal lattice vector). We can mention at once that the carrier (closure) of each trajectory constructed by Tsarev represents a topologically more complex part of the Fermi surface than the two-dimensional tori with holes described in the previous section. As a consequence, the behavior of Tsarev's trajectories on the Fermi surface is more chaotic, and the trajectories themselves can now be assigned to the class of "chaotic" trajectories.

As regards the shape of Tsarev-type trajectories in the extended **p**-space, they actually possess, to some extent, both the properties of stable open trajectories and the properties that are not inherent in stable open trajectories. For example, an open Tsarev's trajectory cannot be enclosed in any straight strip of finite width in the plane orthogonal to **B**. At the same time, for a given direction of the magnetic field, all open Tsarev's trajectories have the same asymptotic direction in the planes orthogonal to **B**, which makes them somewhat similar to stable open trajectories of system (1.1). This property is in fact inherent in all unstable open trajectories arising for partially irrational directions of **B** [34], which allows one to assign all such examples to a class of trajectories of the same type. Moreover, the above-mentioned property of Tsarev's trajectories leads to the fact that the contribution of a part of the Fermi surface carrying such trajectories is also strongly anisotropic in the limit of $\omega_B\tau \gg 1$, just as in the case of open trajectories of system (1.1). In particular, here we also have relation (2.1) for the conductivity tensor in a properly chosen coordinate system. Note, however, that relations (1.4) are no longer satisfied in this case, and the behavior of the conductivity tensor in the case of Tsarev's trajectories becomes somewhat more complex. Note also that, in view of the instability of the trajectories described, the structure of the conductivity tensor is not related here to the topological numbers analogous to those introduced above for stable open trajectories of system (1.1).

The second class of chaotic open trajectories of system (1.1) is given by unstable open trajectories arising for directions of **B** of maximum irrationality. Such trajectories were first constructed by Dynnikov in [34]; these trajectories exhibit maximally chaotic behavior

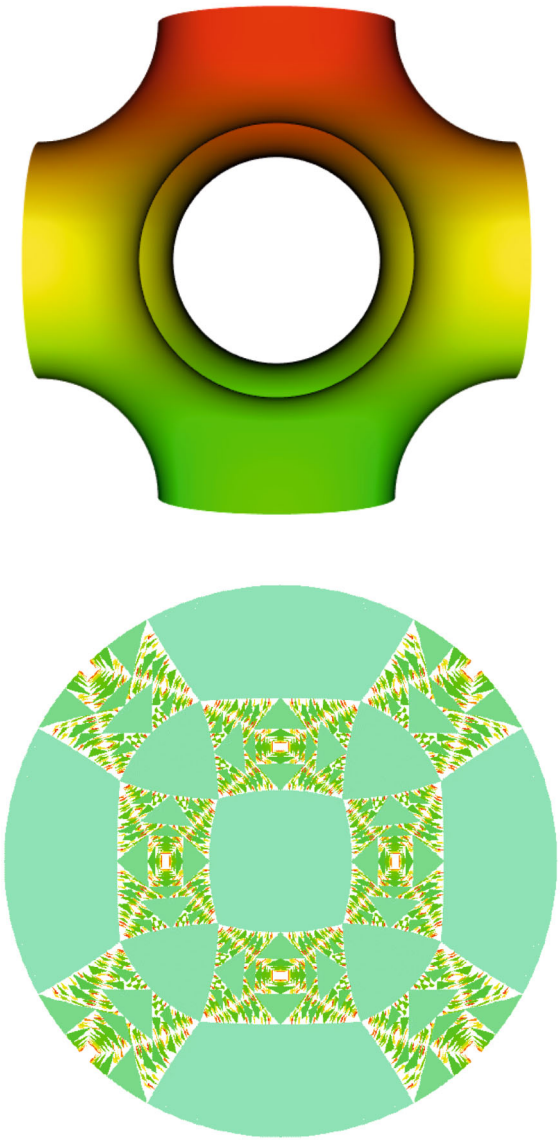

Fig. 14. (Color online) The shape of the surface $\cos x + \cos y + \cos z = 0$ (of genus 3) and the corresponding stability zones on the angular diagram [25, 26].

both on the Fermi surface and in the covering **p**-space (Fig. 15). This property of Dynnikov's trajectories leads to quite nontrivial behavior of the magnetoconductivity tensor in the limit of $\omega_B\tau \gg 1$ when such trajectories appear on the Fermi surface. One of the most interesting features of such behavior is the sharp suppression of conductivity along the magnetic field direction as $\omega_B\tau \to \infty$ [35]. Another specific feature is the appearance of fractional powers of the parameter $\omega_B\tau$ in the asymptotics of the conductivity tensor components [35, 36], which also reflects the specific character of the chaotic dynamics of such trajectories. On the whole, the contribution of the carriers of Dynnikov's chaotic trajectories to all the components of

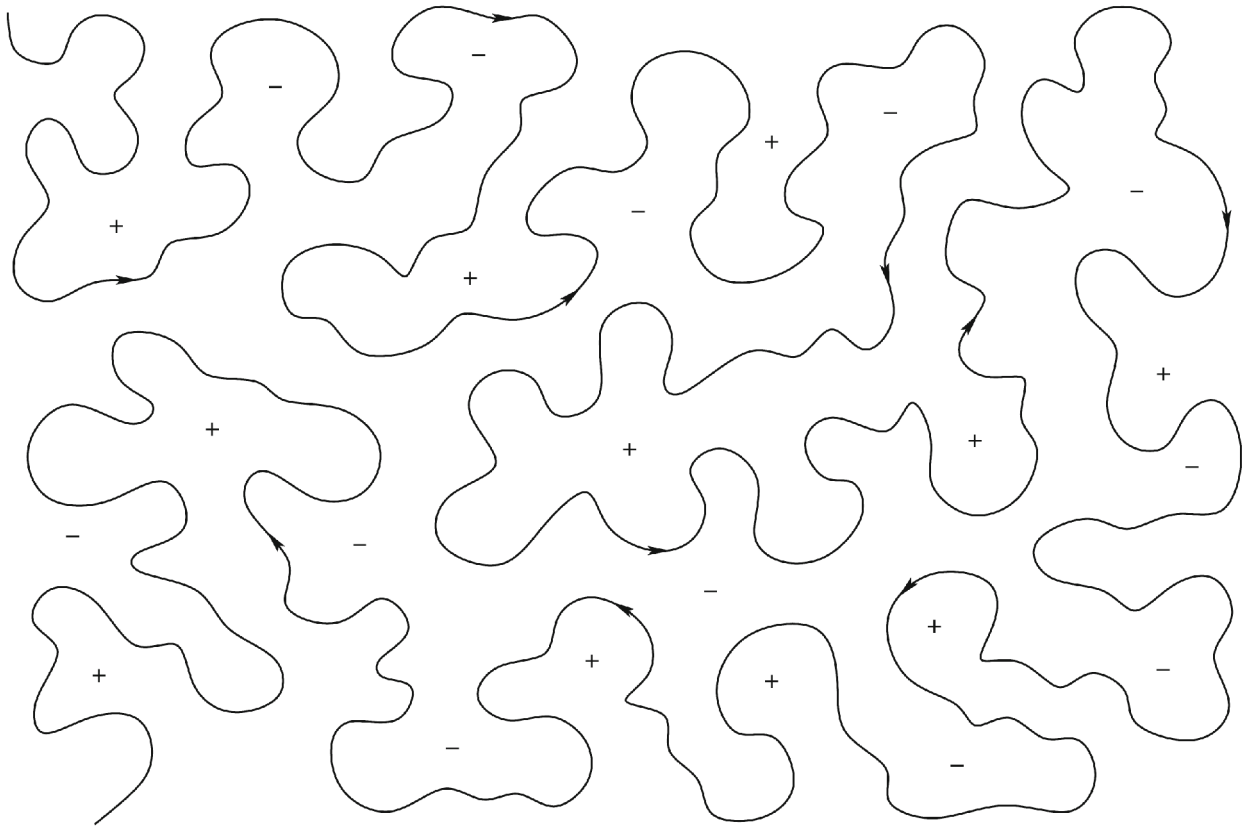

Fig. 15. The form of Dynnikov's chaotic trajectory in the plane orthogonal to **B** in the extended **p**-space.

the conductivity tensor tends to zero in the limit of $\omega_B\tau \to \infty$.

In a somewhat simplified way, we can distinguish two main directions in the study of the chaotic regimes arising in system (1.1), namely, the study of the set of parameters of system (1.1) for which such regimes arise, and the study of specific features of the dynamics of the corresponding chaotic trajectories and the related features of transport phenomena in metals.

To the space of parameters of system (1.1), we can assign the parameters of the dispersion relation $\epsilon(\mathbf{p})$, the Fermi energy ϵ_F, and the direction of the magnetic field **B**. For the most complete theoretical description of system (1.1) for a given dispersion relation $\epsilon(\mathbf{p})$, it is natural to raise the question of the set of directions of **B** corresponding to the appearance of chaotic trajectories on any energy level. As we have already mentioned in the previous section, this set is rather complex and can be described by some fractal structure on the sphere $\mathbb{S}^2$. As we have also already pointed out, according to the Novikov conjecture, the (upper) fractal dimension of this set is strictly less than 2 for generic dispersion relations. The studies of the structure of this set (both analytical and numerical) are currently rather intensive, and one can say that the Novikov conjecture has been largely confirmed at present (see, for example, [41, 42, 44, 50, 53]). Returning to the theory of normal metals, we should also raise the question of the structure of this set for a fixed Fermi level ϵ_F. One can show [19] that the Lebesgue measure of such a set vanishes for a generic Fermi surface. According to the Novikov conjecture [21, 22], the upper Hausdorff dimension of this set in this case is strictly less than one for a generic Fermi surface (although it may be greater for special Fermi surfaces). We can also note that the appearance of chaotic trajectories on the Fermi surface is generally typical of angular diagrams of type B (Fig. 11) mentioned in the previous section, whereas, for angular diagrams of type A, these trajectories may arise only in exceptional cases (see [32]). As we have already said, the studies of the structure of the set of directions of **B** corresponding to the appearance of chaotic trajectories both on a fixed Fermi surface and on any surface of constant energy for a given dispersion law currently represent a rather actively developing branch of topology and the theory of dynamical systems.

The study of the specific features of the dynamics of chaotic trajectories is the most topical in the case of Dynnikov-type trajectories, which exhibit the most complex behavior both on the Fermi surface (in $\mathbb{T}^3$) and in the extended **p**-space. Special examples of such trajectories may have very remarkable properties. For

example, the trajectories constructed in [34] have the property of self-similarity in the **p**-space. Namely, each such trajectory coincides with itself after dilation along some two vectors in the appropriate plane orthogonal to **B** with some eigenvalues, followed by a finite deformation of the trajectory obtained after dilation (isotopy of a trajectory in the plane under which the distance between the initial point of the trajectory and any of its images under the isotopy does not exceed a fixed constant).

Unfortunately, the above-described remarkable property is not inherent in Dynnikov's chaotic trajectories in the general case. However, methods that were initially developed in the abstract theory of dynamical systems and foliations on two-dimensional surfaces (see, for example, [36, 38–40, 45–49]) turned out to be quite effective in the study of the dynamics of such trajectories. In particular, the so-called Zorich–Kontesvich–Forni indices (see, for example, [40]) describing important aspects of the behavior of chaotic trajectories both on the Fermi surface and in the extended **p**-space proved to be quite important characteristics of such trajectories. Here we cannot present a detailed description of the above characteristics; however, we note that they actually play a very important role in the emergence of fractional powers of the parameter $\omega_B\tau$ in the asymptotics of the conductivity tensor components when Dynnikov-type chaotic trajectories appear on the Fermi surface in the general case (see [36]). We can also note that the most comprehensive possible description of the behavior of Dynnikov's chaotic trajectories from the viewpoint of the general theory of dynamical systems is currently a very topical problem, which is of interest for many researchers.

4. CONCLUSIONS

We have presented the latest results of investigations of the problem of dynamics of electronic states on complex Fermi surfaces in the presence of an external magnetic field and their relation to electron transport phenomena in metals in strong magnetic fields. The analysis of transport phenomena in metals has been mainly carried out in the leading (quasiclassical) approximation, which directly relates the specific features of electron dynamics to different regimes of electron transport in the limit of $\omega_B\tau \gg 1$. The results are based on the general theorems of topological character and include the description of all possible types of electron dynamics and the corresponding electron transport regimes in a metal under quite general assumptions about the electron spectrum. At the same time, we have also discussed the problems that are interesting for the further development of this field of research.

FUNDING

This work was supported by the National Science Foundation, project no. DMS-1832126 (R. De Leo), and the Russian Science Foundation, project no. 18-11-00316 (A.Ya. Maltsev).

REFERENCES

1. Ch. Kittel, *Quantum Theory of Solids* (Wiley, New York, 1963; Nauka, Moscow, 1967).
2. J. Ziman, *Principles of the Theory of Solids* (Cambridge Univ. Press, Cambridge, 1976; Mir, Moscow, 1974).
3. A. A. Abrikosov, *Fundamentals of the Theory of Metals* (Nauka, Moscow, 1987; North-Holland, Amsterdam, 1988).
4. I. M. Lifshits, M. Ya. Azbel', and M. I. Kaganov, Sov. Phys. JETP **4**, 43 (1956).
5. I. M. Lifshits and V. G. Peschanskii, Sov. Phys. JETP **8**, 875 (1958).
6. I. M. Lifshits and V. G. Peschanskii, Sov. Phys. JETP **11**, 137 (1960).
7. I. M. Lifshits and M. I. Kaganov, Sov. Phys. Usp. **2**, 831 (1959).
8. I. M. Lifshits and M. I. Kaganov, Sov. Phys. Usp. **5**, 878 (1962).
9. I. M. Lifshits and M. I. Kaganov, Sov. Phys. Usp. **8**, 805 (1965).
10. M. I. Kaganov and V. G. Peschansky, Phys. Rep. **372**, 445 (2002).
11. I. M. Lifshits, M. Ya. Azbel', and M. I. Kaganov, *Electron Theory of Metals* (Nauka, Moscow, 1971; Consultants Bureau, Adam Hilger, New York, 1973).
12. *Conductivity Electrons*, Ed. M. I. Kaganov and V. S. Edel'man (Nauka, Moscow, 1985).
13. S. P. Novikov, Usp. Mat. Nauk **37** (5), 3 (1982).
14. A. V. Zorich, Usp. Mat. Nauk **39**, 235 (1984).
15. I. A. Dynnikov, Usp. Mat. Nauk **47**, 161 (1992).
16. I. A. Dynnikov, Mat. Zam. **53**, 57 (1993).
17. S. P. Novikov and A. Ya. Mal'tsev, JETP Lett. **63**, 855 (1996).
18. S. P. Novikov and A. Ya. Mal'tsev, Phys. Usp. **41**, 231 (1998).
19. I. A. Dynnikov, Usp. Mat. Nauk **54**, 21 (1999).
20. I. A. Dynnikov, in *Surfaces in 3-Torus: Geometry of Plane Sections, Proceedings of ECM2, BuDA, 1996.*
21. A. Ya. Maltsev and S. P. Novikov, Solid State Phys. Bull. Braz. Math. Soc., New Ser. 34, 171 (2003).
22. A. Ya. Maltsev and S. P. Novikov, J. Stat. Phys. **115**, 31 (2004).
23. A. Ya. Maltsev and S. P. Novikov, arXiv:cond-mat/0304471.
24. R. de Leo, SIAM J. Appl. Dynam. Syst. **2**, 517 (2003).
25. R. de Leo, Phys. Lett. A **332**, 469 (2004).
26. R. de Leo, Phys. B (Amsterdam, Neth.) **362**, 62 (2005).
27. R. de Leo, Exp. Math. **15**, 109 (2006).
28. R. de Leo and I. A. Dynnikov, Geom. Dedic. **138**, 51 (2009).
29. A. Ya. Mal'tsev, J. Exp. Theor. Phys. **124**, 805 (2017).

30. A. Ya. Mal'tsev, J. Exp. Theor. Phys. **125**, 896 (2017).
31. A. Ya. Mal'tsev, J. Exp. Theor. Phys. **127**, 1087 (2018).
32. A. Ya. Mal'tsev, J. Exp. Theor. Phys. **129**, 116 (2019).
33. S. P. Tsarev, private commun. (1992–1993).
34. I. A. Dynnikov, Am. Math. Soc. Transl., Ser. 2 179, 45 (1997).
35. A. Ya. Mal'tsev, J. Exp. Theor. Phys. **85**, 934 (1997).
36. A. Ya. Mal'tsev and S. P. Novikov, Tr. MIAN **302**, 296 (2018).
37. A. V. Zorich, in *Proceedings of the Geometric Study of Foliations, Tokyo, November 1993*, Ed. by T. Mizutani et al. (World Scientific, Singapore, 1994), p. 479.
38. A. V. Zorich, Ann. Inst. Fourier 46, 325 (1996).
39. A. Zorich, Am. Math. Soc. Transl., Ser. 2 **179**, 173 (1997).
40. A. Zorich, Am. Math. Soc. Transl., Ser. 2 **197**, 135 (1999).
41. R. De Leo, Usp. Mat. Nauk **55**, 181 (2000).
42. R. De Leo, Usp. Mat. Nauk **58**, 197 (2003).
43. A. Zorich, in *Frontiers in Number Theory, Physics and Geometry*, Vol. 1: *On Random Matrices, Zeta Functions and Dynamical Systems, Proceedings of the Ecole de Physique des Houches, France, March 9–21, 2003* (Springer, Berlin, 2006), p. 439.
44. R. de Leo and I. A. Dynnikov, Usp. Mat. Nauk **62**, 151 (2007).
45. A. Skripchenko, Discrete Contin. Dyn. Sys. **32**, 643 (2012).
46. A. Skripchenko, Ann. Glob. Anal. Geom. **43**, 253 (2013).
47. I. Dynnikov and A. Skripchenko, Am. Math. Soc. Transl., Ser. 2 **234**, 173 (2014); arXiv: 1309.4884.
48. I. Dynnikov and A. Skripchenko, Trans. Moscow Math. Soc. **76**, 287 (2015).
49. A. Avila, P. Hubert, and A. Skripchenko, Invent. Math. **206**, 109 (2016).
50. A. Avila, P. Hubert, and A. Skripchenko, Bull. Soc. Math. (France) **144**, 539 (2016).
51. R. De Leo, in *Advanced Mathematical Methods in Biosciences and Applications,* Ed. by F. Berezovskaya and B. Toni (Springer, 2018); arXiv:1711.01716.
52. A. Ya. Mal'tsev and S. P. Novikov, Usp. Mat. Nauk **74**, 149 (2019).
53. R. Gutiérrez-Romo and C. Matheus. arXiv:1902.04516 [math.DS].
54. Yu. P. Gaidukov, Sov. Phys. JETP **10**, 913 (1959).
55. N. E. Alekseevskii and Yu. P. Gaidukov, Sov. Phys. JETP 15, 49 (1962).
56. I. A. Dynnikov and A. Ya. Mal'tsev, J. Exp. Theor. Phys. **85**, 205 (1997).

Translated by I. Nikitin